Proceedings of the 2009 IEEE International Conference on Mechatronics.
Málaga, Spain, April 2009.

Vibration Reduction in a Flexible Link Mechanism through the Synthesis of an MPC Controller

P. Boscariol, A. Gasparetto and V. Zanotto, *IEEE Member*
Dipartimento di Ingegneria Elettrica, Gestionale e Meccanica, Università di Udine
via delle Scienze 208, 33100 Udine
Email: paolo.boscariol@uniud.it, gasparetto@uniud.it, vanni.zanotto@uniud.it

***Abstract*—The modeling and the control of flexible link robots have received a great deal of attention in the last decades due to the wide prospective industrial and space applications of ultra-light and high-speed mechanisms. This paper introduces a general and practical procedure for the design of effective control schemes for the position and vibration control of flexible links mechanisms. In particular, an innovative controller based on MPC (Model-based Predictive Control) is proposed. So far the MPC controllers have been employed almost exclusively in slow industrial processes. Nevertheless, this work shows that the MPC approach can be successfully adapted to plants whose dynamics are both nonlinear and fast changing as well. The performances of this approach will be evaluated for a single link mechanism and compared to those obtained with a standard PID position controller.**

***Index Terms*—Model Predictive Control, robotics, flexible-link mechanism, vibration, mechatronics**

I. Introduction

Since the early 1970s a great amount of work has been carried out in the field of flexible mechanism modeling, analysis, and control. Admittedly, if it were possible to model and control accurately the vibrational phenomena characterizing flexible mechanisms, it would be also possible to design and build lighter robot manipulators, which in turn would guarantee lower manufacturing and operating costs as long as higher level of productivity thanks to the increased operating speed. Most researchers have focused their investigations on the definition of accurate mathematical models both for single flexible bodies and multi-body systems. Paper [1] presents a comprehensive review of the work done in this area. The most popular approach to flexible mechanism modeling involves the use of discretization methods such as the Finite Element Method (FEM) in order to produce dynamic models with a finite number of elastic degrees-of-freedom. An extensive literature in this field is available in [2-11]. The objective of the present paper is to design and test a Model-based Predictive Controller (MPC) for vibration reduction in a single-link flexible mechanisms. Model Predictive Control refers to a family of control algorithms that compute an optimal control sequence based on the knowledge of the plant and on the feedback information. This kind of control has been first employed in chemical factories to control slow chemical processes, but in recent years has experienced a wider diffusion to other industrial fields [12]. For examples Chen [13] has recently proposed the use of MPC control in a ball mill grinding process, while Perez [14] deals with the control of a rudder roll stabilization system for ships. Other interesting results on MPC control of high-bandwidth systems are [15], [16] and [17]. The availability of more powerful embedded platforms in the last years has encouraged the development of embedded MPC control systems suitable to fast-dynamic plants. For example Hassapis [18] has developed a multicore PC-based embedded MPC control, while FPGA has been chosen by Ling [19] and He [20]. The choice of MPC control for vibrations reduction has been motivated by different factors. First, the prediction ability based on an internal model can be a very effective advantage in fast-dynamic systems. Then MPC is well suited to MIMO plants, since the outputs are computed by solving a minimization problem which can take account of different variables. Moreover, MPC is able to handle constraints on both control and controlled variables. This can be very effective in real-world control strategies where actuators limitations, such as maximum torque, or maximum speed of motors cannot be neglected. The literature on MPC as an effective vibration reduction strategy in flexible systems is very limited, to the authors' knowledge the only papers focusing on this topic are [21], [22] and [23]. Dynamical models used in [21]–[23] are based on modal analysis, while in this paper a more accurate FEM model has been chosen. The MPC controller has been implemented in software simulation and exhaustive tests have been made to prove the accuracy and the effectiveness of this control approach.

II. Dynamic model of a flexible-links planar mechanism

In this section the dynamic model of a flexible-link mechanism proposed by Giovagnoni [10] will be briefly explained. The choice of this formulation among the several proposed in the last 30 years has been motivated mainly by the high grade of accuracy provided by this model, which has been proved several times, for example in [24]–[26]. Each flexible link belonging to the mechanism is divided into finite elements. Referring to Figure 1 the following vectors, calculated in the global reference frame $\{X, Y, Z\}$, can be defined:

- $\mathbf{r}_i$ and $\mathbf{u}_i$ are the vectors of nodal position and nodal displacement in the ith element of the ERLS and of their elastic displacement
- $\mathbf{p}_i$ is the position of a generic point inside the ith element
- $\mathbf{q}$ is the vector of generalized coordinates of the ERLS

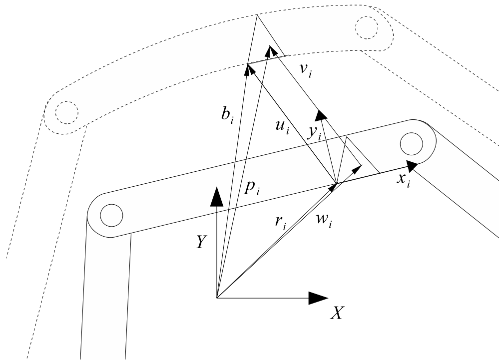

Fig. 1. Kinematic definitions

The vectors defined so far are calculated in the global reference frame $\{X, Y, Z\}$. Applying the principle of virtual work, the following relation can be stated:

$$\begin{aligned}\sum_i \int_{V_i} \delta\mathbf{p}_i{}^T \ddot{\mathbf{p}}_i \rho_i d\nu + \sum_i \int_{V_i} \delta\epsilon_i{}^T \mathbf{D}_i \epsilon_i d\nu \\ = \sum_i \int_{V_i} \delta\mathbf{p}_i{}^T \mathbf{g} \rho d\nu + (\delta\mathbf{u}^T + \delta\mathbf{r}^T)\mathbf{F}\end{aligned} \tag{1}$$

ϵ_i, $\mathbf{D}_i$, ρ_i and $\delta\epsilon_i$ are, respectively, the strain vector, the stress-strain matrix, the mass density and the virtual strains of the ith link. $\mathbf{F}$ is the vector of the external forces, including the gravity, whose acceleration vector is $\mathbf{g}$. Eq. 1 shows the virtual works of, respectively, inertia, elastic an external forces. From this equation, $\delta\mathbf{p}_i$ and $\ddot{\mathbf{p}}_i$ for a generic point in the ith element are:

$$\begin{aligned}\delta\mathbf{p}_i &= \mathbf{R}_i \mathbf{N}_i \mathbf{T}_i \delta\mathbf{r}_i \\ \ddot{\mathbf{p}}_i &= \mathbf{R}_i \mathbf{N}_i \mathbf{T}_i + 2(\dot{\mathbf{R}}_i \mathbf{N}_i \mathbf{T}_i + \mathbf{R}_i \mathbf{N}_i \dot{\mathbf{T}}_i)\dot{\mathbf{u}}_i\end{aligned} \tag{2}$$

where $\mathbf{T}_i$ is a matrix that describes the transformation from global-to-local reference frame of the ith element, $\mathbf{R}_i$ is the local-to-global rotation matrix and $\mathbf{N}_i$ is the shape function matrix. Taking $\mathbf{B}_i(x_i, y_i, z_i)$ as the strain-displacement matrix, the following relation holds:

$$\delta\epsilon_i = \mathbf{B}_i \delta\mathbf{T}_i \mathbf{u}_i + \mathbf{B}_i \mathbf{T}_i \delta\mathbf{u}_i \tag{3}$$

Since nodal elastic virtual displacements ($\delta\mathbf{u}$) and nodal virtual displacements of the ERLS ($\delta\mathbf{r}$) are independent from each other the resulting equation describing the motion of the system is:

$$\begin{bmatrix} \mathbf{M} & \mathbf{MS} \\ \mathbf{S}^T\mathbf{M} & \mathbf{S}^T\mathbf{MS} \end{bmatrix} \begin{bmatrix} \ddot{\mathbf{u}} \\ \ddot{\mathbf{q}} \end{bmatrix} = \begin{bmatrix} \mathbf{f} \\ \mathbf{S}^T\mathbf{f} \end{bmatrix} \tag{4}$$

$\mathbf{M}$ is the mass matrix of the whole system and $\mathbf{S}$ is the sensitivity matrix for all the nodes. Vector $\mathbf{f} = \mathbf{f}(\mathbf{u}, \dot{\mathbf{u}}, \mathbf{q}, \dot{\mathbf{q}})$ takes account of all the forces affecting the system, including the gravity force. Adding a Rayleigh damping, the right-hand side of Eq. 4 becomes:

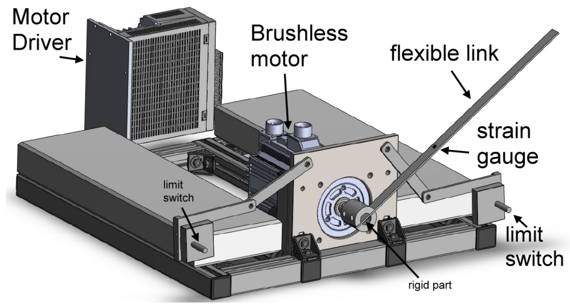

Fig. 2. The reference mechanism

$$\begin{aligned}\begin{bmatrix} \mathbf{f} \\ \mathbf{S}^T \end{bmatrix} = \begin{bmatrix} -2\mathbf{M}_G - \alpha\mathbf{M} - \beta\mathbf{K} & -\mathbf{M}\dot{\mathbf{S}} & -\mathbf{K} \\ \mathbf{S}^T(-2\mathbf{M}_G - \alpha\mathbf{M}) & -\mathbf{S}^T\mathbf{M}\dot{\mathbf{S}} & 0 \end{bmatrix} \begin{bmatrix} \dot{\mathbf{u}} \\ \dot{\mathbf{q}} \\ \mathbf{u} \end{bmatrix} \\ + \begin{bmatrix} \mathbf{M} & \mathbf{I} \\ \mathbf{S}^T\mathbf{M} & \mathbf{S}^T \end{bmatrix} \begin{bmatrix} \mathbf{g} \\ \mathbf{F} \end{bmatrix}\end{aligned} \tag{5}$$

Matrix $\mathbf{M}_G$ accounts for the Coriolis contribution, while $\mathbf{K}$ is the stiffness matrix of the whole system. α and β are the two Rayleigh damping coefficients. The system in (4) and (5) can be made solvable by forcing to zero as many elastic displacement as the generalized coordinates, in this way ERLS position is defined univocally [10]. Finally, after removing the displacement forced to zero from (4) and (5) one obtains:

$$\begin{bmatrix} \mathbf{M}_{in} & (\mathbf{MS})_{in} \\ (\mathbf{S}^T\mathbf{M})_{in} & \mathbf{S}^T\mathbf{MS} \end{bmatrix} \begin{bmatrix} \ddot{\mathbf{u}}_{in} \\ \ddot{\mathbf{q}} \end{bmatrix} = \begin{bmatrix} \mathbf{f}_{in} \\ \mathbf{S}^T f \end{bmatrix} \tag{6}$$

III. Reference Mechanism

The mechanism under analysis is shown in Figure 2. A torque-controlled brushless motor moves a flexible link arm on the vertical plane. Both the mechanical and geometric parameters of the flexible bar have been provided in Table I. The coupler with the motor shaft is considered perfectly rigid.

The flexible link has been modeled using two finite elements (Figure 3). The first part of the link which, in the real mechanism, is screwed inside the joint is considered to be rigid. The generalized coordinate of the ERLS is the angle q at the motor shaft.

The total number of elastic degrees of freedom is 9, but two of them must be forced to zero in order to take account of the hinge on the first node. It is necessary to force to zero another elastic degree of freedom in order to produce a valid ERLS model, as it has been stated in [10]. A suitable choice is to set to zero the rotation in the first node.

The resulting system is described by 6 nodal elastic displacements and one rigid degree of freedom, as represented in Figure 3.

A. Linearized model

The dynamic model represented by (6) is strongly nonlinear, due to the quadratic relation between the nodal accelerations and the velocities of the free coordinates, and to the effects

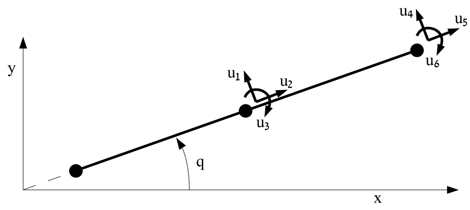

Fig. 3. Elastic displacements in the flexible link mechanism

TABLE I
KINEMATIC AN DYNAMIC CHARACTERISTICS OF REFERENCE MECHANISM

	symbol	value
Young's modulus	E	$210 \cdot 10^{9}$ [Pa]
Flexural inertia moment	J	$11.102 \cdot 10^{-10}$ $[m^4]$
Beam width	a	$30 \cdot 10^{-3}$ [m]
Beam thickness	b	$5 \cdot 10^{-3}$ [m]
Beam mass/unit	m	$272 \cdot 10^{-3}$ $[Kg/m]$
Length of rigid part	L_1	0.047 [m]
Length of flexible part	L_2	0.653 [m]
Rayleigh damping constants	α	$8.72 \cdot 10^{-2}$ $[s^{-1}]$
	β	$2.1 \cdot 10^{-5}$ [s]

of the gravity force. Thus it cannot be used as a prediction model for a linear MPC controller. In order to develop a state-space form linearized version of the dynamic system of (6) a linearization procedure has been developed by Gasparetto in [28]. Here this procedure will be briefly recalled.

From the basics of system theory, a linear time-invariant model expressed in state-space can be written as:

$$\begin{cases} \dot{\mathbf{x}}(t) = \mathbf{F}_{lin}\mathbf{x}(t) + \mathbf{G}_{lin}\mathbf{v}(t) \\ \mathbf{y}(t) = \mathbf{H}_{lin}\mathbf{x}(t) + \mathbf{D}_{lin}\mathbf{v}(t) \end{cases} \tag{7}$$

where $\mathbf{x}(t)$ is the state vector, $\mathbf{y}(t)$ is the output vector, $\mathbf{v}(t)$ represents the input vector and $\mathbf{F}_{lin}$, $\mathbf{G}_{lin}$, $\mathbf{H}_{lin}$ and $\mathbf{D}_{lin}$ are time-invariant matrices. Taking $\mathbf{x} = [\dot{\mathbf{u}}, \dot{\mathbf{q}}, \mathbf{u}, \mathbf{q}]^T$ as the state vector, linearized state-space form of the dynamic model in (6) can be written as:

$$\mathcal{A}_{lin}\dot{\mathbf{x}} = \mathcal{B}_{lin}\ \mathbf{x} + \mathcal{C}_{lin}\tau \tag{8}$$

Now a steady "equilibrium" configuration $\mathbf{x}_e$ where $\mathbf{u} = \mathbf{u}_e$ under the system input $\mathbf{v} = \mathbf{v}_e$ can be chosen. In the neighborhood of this point holds:

$$\begin{cases} \mathbf{x}(t) = \mathbf{x}_e + \Delta\mathbf{x}(t) \\ \mathbf{v}(t) = \mathbf{v}_e + \Delta\mathbf{v}(t) \end{cases} \tag{9}$$

So, bringing these relations into (6), the following relationship turns out:

$$\mathcal{A}_{lin}(\mathbf{x}_e)\Delta\dot{\mathbf{x}} = \mathcal{B}_{lin}(\mathbf{x}_e{+}\Delta\mathbf{x})(\mathbf{x}_e{+}\Delta\mathbf{x}){+}\mathcal{C}_{lin}(\mathbf{x}_e{+}\Delta\mathbf{x})(\mathbf{v}_e{+}\Delta\mathbf{x}) \tag{10}$$

After some steps that can be found in more detail in [28], $\mathcal{A}_{lin}$ and $\mathcal{B}_{lin}$ matrices in (8) can be written as:

$$\mathcal{A}_{lin} = \begin{bmatrix} \mathbf{M} & \mathbf{MS} & \mathbf{0} & \mathbf{0} \\ \mathbf{S}^T\mathbf{M} & \mathbf{S}^T\mathbf{MS} & \mathbf{0} & \mathbf{0} \\ \mathbf{0} & \mathbf{0} & \mathbf{I} & \mathbf{0} \\ \mathbf{0} & \mathbf{0} & \mathbf{0} & \mathbf{I} \end{bmatrix} \tag{11}$$

$$\mathcal{B}_{lin} = \begin{bmatrix} -2\mathbf{M}_G - \alpha\mathbf{M} - \beta\mathbf{K} & \mathbf{0} & -K & \mathbf{B}_{14} \\ \mathbf{S}^T(-2\mathbf{M}_G - \alpha\mathbf{M} - \beta\mathbf{K}) & \mathbf{0} & \mathbf{0} & \mathbf{B}_{24} \\ \mathbf{I} & \mathbf{0} & \mathbf{0} & \mathbf{0} \\ \mathbf{0} & \mathbf{I} & \mathbf{0} & \mathbf{0} \end{bmatrix} \tag{12}$$

where: $\mathbf{B}_{14} = -\left.\frac{\partial\mathbf{K}}{\partial\mathbf{q}}\right|_{\mathbf{q}=\mathbf{q}_e} \cdot \mathbf{u}_e + \left.\frac{\partial\mathbf{f}_g}{\partial\mathbf{q}}\right|_{\mathbf{q}=\mathbf{q}_e}$
and $\mathbf{B}_{24} = \left.\frac{\partial\left(\mathbf{S}^T\mathbf{f}_g\right)}{\partial\mathbf{q}}\right|_{\mathbf{q}=\mathbf{q}_e}$.

$\mathcal{C}_{lin}$ remains unchanged after the linearization process, since it is composed of only zeros and ones. The standard form of the state-space system can be easily found from $\mathcal{A}_{lin}$, $\mathcal{B}_{lin}$ and $\mathcal{C}_{lin}$:

$$\begin{aligned} \Delta\dot{\mathbf{x}} &= \mathbf{F}_{lin}\Delta\mathbf{x} + \mathbf{G}_{lin}\Delta\mathbf{v} \\ \mathbf{y} &= \mathbf{H}_{lin}\mathbf{x} + \mathbf{D}_{lin}\mathbf{v} \end{aligned} \tag{13}$$

where:

$$\begin{aligned} \mathbf{F}_{lin} &= {\mathcal{A}_{lin}}^{-1}\mathcal{B}_{lin} \\ \mathbf{G}_{lin} &= {\mathcal{A}_{lin}}^{-1}\mathcal{C}_{lin} \end{aligned} \tag{14}$$

Since the state vector $\mathbf{x}$ is measured in the global reference frame, in order to get the output vector $\mathbf{y}$ with nodal displacements in the local reference frame, a global-to-local rotation matrix $\mathbf{T}_{LG}(q)$ must be used.

In oder to get the displacements measured in the local reference frame and q as the outputs of the state-space model, the following $\mathbf{H}_{lin}$ matrix has to be used:

$$\mathbf{H}_{lin} = \left[\mathbf{0}^{[7\times1]} \;\middle|\; \begin{matrix} \mathbf{T}_{LG}(q_e)^{[6\times6]} & \\ & 1 \end{matrix}\right] \tag{15}$$

$\mathbf{D}_{lin}$ matrix is composed by only zeros and ones, since the only external force is the torque provided by the actuator and its sensitivity coefficient is 1.

B. Accuracy of the linearized model

In order to demonstrate the level of accuracy of the linearized model, a comparison based on the impulsive response of the mechanism was set. To do this, the mechanism was with a 5 Nm torque impulse together with a contribute to compensate gravity effects. The initial configuration has been arbitrarily chosen as $q_0 = 0$, but the effectiveness of the linearization model holds for any configuration of choice. Here the results on transverse nodal displacements u_2 and angular position q is shown, but the likeness of the linearized and nonlinear model extends also to all the other 5 nodal displacements belonging to the model.

As can be seen from the two graphs in Figure 4 and 5, the linearized model presents a very high level of accuracy. As long as the mechanism moves in a limited range from its "equilibrium" configuration the response of the two models are virtually identical, but moving outside a safety range of ±0.3 rad some discrepancies between the two model arises. As stated in [28], the steady-state error in a similar system is limited to 3% up to a 1.2 rad angular displacement.

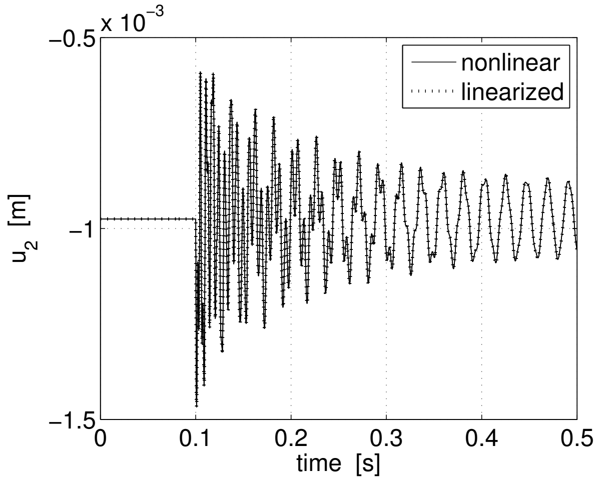

Fig. 4. Comparison of the nonlinear vs. linearized system impulsive response: nodal displacement u_2 along the local y-axis

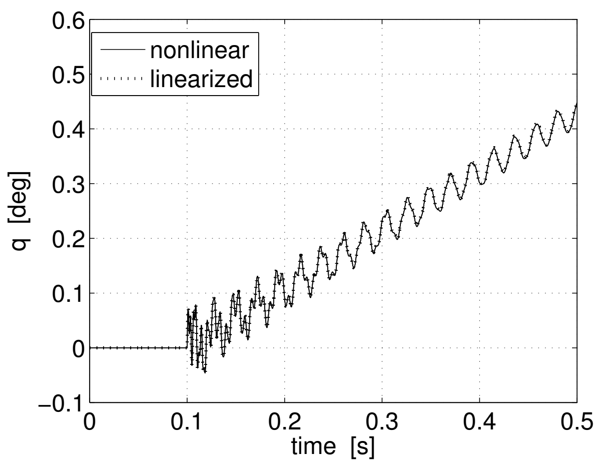

Fig. 5. Comparison of the nonlinear vs. linearized system impulsive response: angular position q

IV. MODEL PREDICTIVE CONTROL WITH CONSTRAINTS

In this section the equations leading to the constrained MPC system employed will be briefly analyzed. Basically, MPC control law is calculated as an optimization problem, whose evolution is influenced by both the plant actual input/outputs and its estimated future behavior. In this section a very brief explanation of those concepts is given, more details can be found in [27].

A. Model prediction

Given a plant model in state-space form:

$$\begin{cases} \mathbf{x}(k+1) = \mathbf{F}\mathbf{x}(k) + \mathbf{G}\mathbf{u}(k) \\ \mathbf{y}(k) = \mathbf{H}\mathbf{x}(k) \end{cases} \tag{16}$$

where $\mathbf{x}(k)$ is the state vector, $\mathbf{u}(k)$ and $\mathbf{y}(k)$ are the input and output vectors, respectively. Assuming that the whole state $\mathbf{x}(k)$ is measured, the future behavior of the plant at time k over H_p steps, indicated by $[\hat{\mathbf{x}}(k+1|k), \ldots, \hat{\mathbf{x}}(k+H_p|k)]$, can be evaluated as:

$$\begin{aligned} &\hat{\mathbf{x}}(k+1|k) = \mathbf{F}\mathbf{x}(k) + \mathbf{G}\hat{\mathbf{u}}(k|k) \\ &\hat{\mathbf{x}}(k+2|k) = \mathbf{F}\hat{\mathbf{x}}(k+1|k) + \mathbf{G}\hat{\mathbf{u}}(k+1|k) \\ &\vdots \\ &\hat{\mathbf{x}}(k+H_p|k) = \mathbf{F}\hat{\mathbf{x}}(k+H_p-1|k) + \mathbf{G}\hat{\mathbf{u}}(k+H_p-1|k) = \\ &= \mathbf{F}^{H_p}\mathbf{x}(k) + \mathbf{F}^{H_p-1}\mathbf{G}\hat{\mathbf{u}}(k|k) + \ldots + \mathbf{G}\hat{\mathbf{u}}(k+H_p-1|k) \end{aligned} \tag{17}$$

Prediction values of outputs are calculated from predicted states:

$$\hat{\mathbf{y}}(k+n|k) = \mathbf{H}\hat{\mathbf{x}}(k+n|k); \qquad n = 1, 2, \ldots, H_p \tag{18}$$

B. Constrained optimization solution

We suppose to have constraints on both control and controlled variables ($u_i(k)$ and z_i(k)) respectively), and on their change rate ($\Delta u_i(k)$), in terms of linear inequalities, such as:

$$u_{imin} \le u_i(k) \le u_{imax} \tag{19}$$

$$\Delta u_{imin} \le \Delta u_i(k) \le \Delta u_{imax} \tag{20}$$

$$z_{imin} \le z_i(k) \le z_{imax} \tag{21}$$

Those inequalities can be expressed as in matrix form:

$$\mathbf{V_1} \begin{bmatrix} \mathcal{U}(k) \\ 1 \end{bmatrix} \le 0 \tag{22}$$

$$\mathbf{V_2} \begin{bmatrix} \Delta\mathcal{U}(k) \\ 1 \end{bmatrix} \le 0 \tag{23}$$

$$\mathbf{V_3} \begin{bmatrix} \mathcal{Z}(k) \\ 1 \end{bmatrix} \le 0 \tag{24}$$

$\mathcal{U} = \left[\hat{\mathbf{u}}(k|k)^T, \ldots, \hat{\mathbf{u}}(k+H_u-1|k)^T\right]^T$, $\Delta\mathcal{U}$ and $\mathcal{Z}$ are the vectors of estimated input values, input change rate and controlled viables, respectively. A similar relation can be used to express also $\Delta\mathcal{U}$. $\mathcal{Z}(k)$ can be calculated as in [27]:

$$\mathcal{Z}(k) = \Psi\hat{\mathbf{x}}(k|k) + \Upsilon\mathbf{u}(k-1) + \Theta\Delta\mathcal{U}(k) \tag{25}$$

which results from a different matricial rearrangement of (17). Without going into further details, (23-25) can be put together in a single inequality:

$$\begin{bmatrix} \Xi \\ \Gamma\Theta \\ \mathbf{W} \end{bmatrix} \Delta\mathcal{U}(k) \le \begin{bmatrix} -\Xi_i\mathbf{u}(k-1) - \mathbf{f} \\ -\Gamma\left[\Psi\mathbf{x}(k) + \Upsilon\mathbf{u}(k-1)\right] - \mathbf{g} \\ \mathbf{w} \end{bmatrix} \tag{26}$$

where Ξ, Ξ_i and $\mathbf{f}$ are a subset of $\mathbf{V_2}$ such that $\mathbf{V_2} = [\Xi, \mathbf{f}] = \left[\Xi_i, \ldots, \Xi_{H_p}, \mathbf{f}\right]$, while $\mathbf{V_3}$ can be split as: $\mathbf{V_3} = [\Gamma, \mathbf{g}]$. $\mathbf{W}$ and $\mathbf{w}$ result from a different formulation of inequality (21), namely:

$$\mathbf{W}\Delta\mathcal{U}(k) \le \mathbf{w} \tag{27}$$

Once all inequality constraints are collected in a single formula, as in (27), the focus can be set on the minimization problem, which can be formulated as:

$$\min_{\Delta\mathcal{U}(k)} \Delta\mathcal{U}(k)^T \mathcal{H} \Delta\mathcal{U}(k) - \mathcal{G}^T \Delta\mathcal{U}(k) \tag{28}$$

subject to constraint (27). This minimization problem is a standard QP (quadratic programming) problem, since it is in the form: $\min_{\theta} \frac{1}{2}\theta^T \Phi \theta + \phi^T \theta$ with $\Omega\theta \leq \omega$. Moreover, this problem is convex ([27]), i.e. there are no local minima.

Some of the equations shown above contain the state vector **x**, but in practical applications it is impossible to measure all the 6 nodal displacements (and their time derivatives) belonging to the state vector. Hence the need of the state observer to obtain an estimation of the full state vector from a subset of it. Here a standard Kalman asymptotic estimator has been used. Matrix **L** is chosen in order to minimize the mean square error between the estimated and the actual values of the state variable. Being the problem fully observable, **L** is calculated as:

$$\mathbf{L} = \mathbf{P}_k \mathbf{H}^T \mathbf{U}_k{}^{-1} \tag{29}$$

where $\mathbf{P}_k$ is the solution of the Riccati equation: $\mathbf{E}\mathbf{P}_k + \mathbf{P}_k\mathbf{E}^T - \mathbf{P}_k\mathbf{H}^T\mathbf{U}_k{}^{-1}\mathbf{H}\mathbf{P}_k + \mathbf{Q}_k = 0$, where $\mathbf{U}_k$ and $\mathbf{Q}_k$ are the measurement and process noise covariance matrices ([29]). In this way the state observer can get an accurate estimation of the full state **x** from the knowledge of u_9, u_{10} and q.

V. Results of the Model Predictive Controller

Here the results obtained in simulation employing a PID position control and an MPC simultaneous control of both vibration and angular position of the mechanism are presented. This controller acts as an MISO (Multiple-Input, Single-Output) system: it relies on the knowledge of the instantaneous values of displacements u_2 and link angular position q. u_2 and q are the two controlled variables, while the torque applied to the mechanism acts as the control variable. So the tuning of the MPC depends on 5 variables: weight w_2 on u_2 , weight w_q on q , sampling time T_s, prediction horizon H_p and control horizon H_c. Then the constraints on both control and controlled variables should be taken into account. Here the following inequality constraints have been used:

$$u_{2_{min}} \leq u_2 \leq u_{2_{min}} \quad q_{min} \leq q \leq q_{min} \quad \tau_{min} \leq \tau \leq \tau_{min}$$

The overall behavior of the controller depends on a large set of variables. While τ_{min} and τ_{max} depend on actuator peak torque, all the others parameters can be tuned quite freely. As a simple rule of thumb, the inequality constraints should be chosen considering the desired performance of the closed-loop system, but always taking care of not setting them too tight, otherwise the system may behave unexpectedly.

Other parameters whose values have a strong influence on the closed-loop dynamic behavior are the prediction horizon H_p and the control horizon H_c. Values of T_s, H_p and H_c should be chosen, in practical applications, according to the available computational resources. Every choice of T_s requires to solve the optimization problem $1/T_s$ times every second, and the computational cost of every evaluation is directly proportional both to H_p and H_c. Here $T_s = 10$ ms has been chosen as a tradeoff between the performance and the need for computational resources. Referring to [19], Ling proved that a 1.5 million gates FPGA can handle values of T_s around 20 ms using high-level FPGA programming without any particular optimization strategy. On the other side, Bleris in [15] proved that using more specialized hardware and optimization techniques allows to set T_s as low as 1 ms.

A. *MPC control performances*

Here a comparison between the system performance under PID and MPC is set. As it can be seen from figure 6, MPC provides a big step forward in vibration damping. Lateral displacement is effectively damped in a very short time (about 250 ms), and the reference position is being tracked with a remarkably high precision and speed: in roughly 200 ms the mechanism can reach its final position showing a very limited overshoot. This overshoot is also dramatically reduced in comparison to PID control [30]: the ability of MPC to predict the future behavior of the system allows to reduce the spring-back effects of the flexible link that usually arises when a flexible element is subject to high angular accelerations.

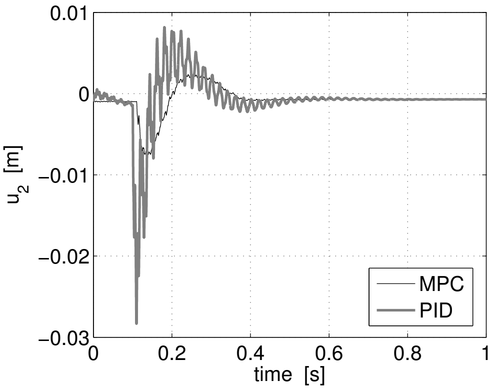

Fig. 6. Transverse vibration u_2 at the mid-point of the follower link, comparison between PID and MPC control system

VI. Conclusion

A high-accuracy FEM-based dynamical model of a single-link mechanism with both rigid and flexible elements has been presented in this paper. Since the elastic beam rotates in the vertical plane, the effects of gravity have been accurately taken into account. This model has been employed in software simulation environment to investigate the effectiveness of Model-based Predictive Control (MPC) with constraints for vibration damping in flexible mechanisms during high-speed rotations. In order to implement the control system, a linearized model of the dynamic system has been developed. This linearized state-space model is capable of a high precision approximation of mechanism dynamic behavior, on both position and vibration dynamics. The performances this control systems is compared

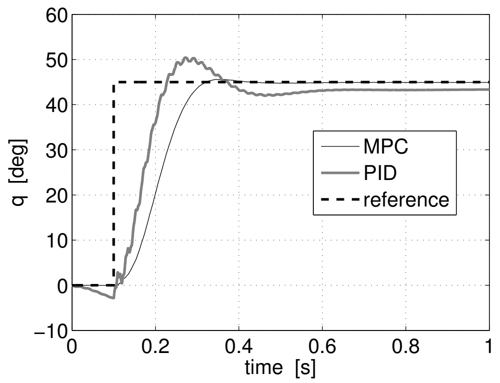

Fig. 7. Crank position q, comparison between PID and MPC control system

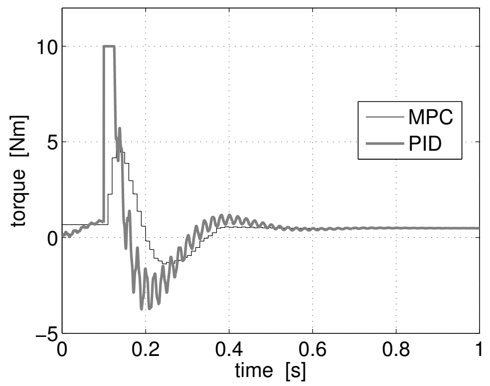

Fig. 8. Applied torque: comparison between PID and MPC control system

to the ones that can be obtained trough a standard PID control. MPC control proved to be very effective both for reference position tracking and vibration suppression.

REFERENCES

[1] S. K. Dwivedy, P. Eberhard, Dynamic analysis of flexible manipulators, a literature review. *Mechanism and Machine Theory* 41, 749-777 (2006)

[2] G.G. Lowen, W.G. Jandrasits: Surevey of investigation into the dynamic behaviour of mechanism containing links with distributed mass and elasticity. *Mech Mach Theory* 7, 3-17 (1972)

[3] A.G. Erdamin, G.N. Sandor: Kineto-elastodynamics: a review if the state-of the-art and trends. *Mech Mach Theory* 7, 19-33 (1972)

[4] G.G. Lowden, C.C. Chassapis: The elastic behaviour of linkages: an update. *Mech Mach Theory* 21, 33-42 (1986)

[5] D.A. Turcic, A. Midha: Generalized equations of motion for the dynamic analysis of elstic mechanism systems. *ASME J Dyn Syst Meas Control* 106, 242-248 (1984)

[6] F.W. Liou, A.G. Erdman: Analysis of a high-speed flexible four-bar linkage: Part I: formulation and solution. *ASME J Vib Acoust Stress. Reliable Design* 111, 35-41 (1989)

[7] S. Nagarayn, D.A. Turcic: Lagrangian formulation of the equation with mutual dependence between rigid body and elastic motions. Part I: element equations. *ASME J Dyn Syst Meas Control* 112, 203-214 (1990)

[8] S. Nagarayn, D.A. Turcic: Lagrangian formulation of the equation with mutual dependence between rigid body and elastic motions. Part II: system equations. *ASME J Dyn Syst Meas Control* 112:215-224 (1990)

[9] B. Jonker: Linearization of dynamic equations of flexible mechanisms: a finite element approach. *Int J Num Methods Eng* 31,1375-1392 (1991)

[10] M. Giovagnoni, A numerical and experimental analysis of a chain of flexible bodies, *Journal of Dynamic Systems, Measurement, and Control* 113, 73-80 (1994)

[11] K.M. Hsiao, R.T. Yang: Effect of member initial curvature on a flexible mechanism response. *J Sound Vib* 190, 315-322 (1996)

[12] S. J. Qin, T. A. Baggwell, A survey of industrial model predictive control technology, *Control Engineering Pratice* 11, 733-764 (2003)

[13] Xi-song Chen, Qi Li, Shu-min Fei, Constrained model predictive control in ball mill grinding process, *Powder Technology* 186, 31-39 (2008)

[14] T. Perez, G.C. Goodwin, C.W. Tzeng, Model predictive rudder roll stabilization control for ships, *Proc. 5th IFAC Conf. on Manouvering and Control of Marine Craft*, (2000), Aalborg, Denmark

[15] L. Bleris, J. Garcia, M. Kothare, Model predictive Hydrodynamic Regulations of Microflows, *American Control Conference*, Portland, OR, June 8-10 2005, 1752-1757

[16] M. Morari, M. Baotić, F. Borrelli, Hybrid systems modeling and control, *European Journal of Control* 9, 177-27 (2003)

[17] R.M. Murray, J. Hauser, A. Jadbabie, M.B. Milam, N. Petit, W.B. Dunbar, R. Franz, Online control customization via aptimization-based control, *Software-Enabled Control* (T. Samad and G. Balas Eds.), (2003) IEEE Press and Wiledy

[18] G. Hassapis, Implementation of model predictive control using real-time multiprocessing computer, *Multiporcessor and Microsystems* 27, 327-340 (2003)

[19] K. V. Ling, S.P. Yue, J. Maciejowski, A FPGA implementation of model predictive control, in proceedings of *American Control Conference*, 14-16 June 2006

[20] M. He, C. Chen, X. Zhang, FPGA Implementation of a Recursive Rank One Updating Matrix Inversion Algorithm for Constrained MPC, *Intelligent Control and Automation* 1, 733-737 (2006)

[21] M. Hassan, R. Dubay, C. Li, R. Wang, Active vibration control of a flexible one-link manipulator using a multivariable predictive controller *Mechatronics* 17, 311-323 (2007)

[22] I.A. Shiptico, K.V. Zmeu, Predictive Controller Deisgn for Flexible-link manipulator, *Proceedings of Modern Technique and Technologies 2002*

[23] K. Zmeu, E. Shiptico, Predictive controller design with offline model learning for flexible beam control, *Proceedings of Physics and Control, 2005.*

[24] A. Gasparetto, V. Zanotto, Vibration reduction in a flexible-link mechanism trough synthesis of an optimal controller. *Meccanica* 41, 611-622 (2006)

[25] A. Gasparetto, On the modeling of flexible-link planar mechanisms: experimental validation of an accurate dynamic model, *Journal of Dynamic Systems, Measurement, and Control* 126 (2004) 365-375

[26] R. Caracciolo, E. Ceresole, M. Giovagnoni, Control experiment of a flexible robot arm using the floating frame model. *Journal of Robotics and Mechatronics* 8, 112-121 (1996)

[27] J. M. Maciejowski, Predictive Control with Constraints. Prentice Hall (2002)

[28] A. Gasparetto, Accurate modeling of a flexible-link planar mechanism by means of a linearized model in the state-space form for design of a vibration control. *Journal of sound and vibration*, vol. 240, no2, pp. 241-26 (2001)

[29] F.G. Franklin, J.D. Powell, M.L. Workman, Digital Control of dynamic systems. 2nd ed. Addison Wesley (1990)

[30] P. Boscariol, A. Gasparetto, A. Lanzutti, R. Vidoni, V. Zanotto, FLIMHILS: A Harware-In-the-Looop Simulator of Flexible Links Mechanisms, *Acta Mechanica Slovaca*, 2-A, 81-94 (2008)